DURABILITY OF TRI-AXIALLY WOVEN FABRIC COMPOSITES FOR SPACE APPLICATIONS

T. Aoki[1]*, Y. Kosugi[1], A. Watanabe[2], T. Murakami[3]
[1] Department of Aeronautics and Astronautics, University of Tokyo, Tokyo, Japan,
[2] Sakase Adtech Co. Ltd., Maruoka, Japan
[3] Industrial Technology Center of Fukui Prefecture, Fukui, Japan
* Corresponding author (aoki@aastr.t.u-tokyo.ac.jp)

Keywords: *Tensile fatigue, Cyclic loading, Failure mechanism, Debonding, Creep, CT scan.*

1 Introduction

Triaxially-woven fabric (TWF) composite is a distinctive type of composite system made up of three sets of inter-woven tows placed in three equally distributed in-plane directions combined with the matrix resin impregnated in the tows. TWF composite has a number of advantageous features such as low apparent density, quasi-isotropy in stiffness, and high flexibility, all of which come from its unique contexture. In addition, low thermal sensitivity of the TWF composite comprising of carbon fibers is of great advantage especially for space structures. Research works have been intensively conducted to investigate stiffness characteristics of TWF composite analytically and experimentally[1-6]. In these studies, the fundamental mechanical behaviors have been predicted through numerical simulations either with finite element model or beam network model, and experiments have shown that the analytical solutions fit sufficiently well with experimental results.

TWF composite has been utilized in several components of space structures such as parabolic antennas[7-10]. Mars-orbiting aeronomy probe "Nozomi[7] (Planet-B)" was the first Japanese satellite that made use of TWF composite for its antenna. Asteroid sample return spacecraft "Hayabusa[8] (Musec-C)" also equipped with an antenna made of TWF composite. "SPINAR (Space Inflation Actuated Rod)" [9] was Japan's first space verification experiment of a space-inflatable assisted extendible structure which made a full use of TWF composite as its extendible rod.

Over the past decades, many researchers have studied the design and construction methods of large space structures, and among them inflatable membrane structure has been considered to be one of the most advantageous options. The group including part of the authors has been preparing to conduct a series of experiments to verify the feasibility of inflatable structural components which may be essential for part of the future space programs. The project named "Space Inflatable Membrane structure Pioneering Long-term Experiments[11] (SIMPLE)" is currently underway for scheduled launch to the International Space Station in 2012. As one of the advantages of TWF composite is high flexibility, the project team focuses on the favorable features of this composite when used as the major load-carrying material of inflatable structures. The TWF composite is utilized in the inflatable extensible mast equipment to demonstrate its high adaptability to deployable or inflatable structures. The material system will also be exposed to the orbital environment and the possible degradation will be monitored. Taking into account that the inflatable structures may be set up in orbit for extended period of time, fatigue effects of TWF composite under mechanical or thermal loadings may not be dismissed and may even be critical to the structural design. Most of the existing studies focus on its stiffness characteristics and let alone its fracture mechanisms.

In this study, fatigue life characteristic, along with damage propagation and accumulation mechanisms of TWF composite are experimentally investigated. To predict fatigue life features, fatigue experiments are conducted to acquire S-N curves. Damage propagation and accumulation mechanisms are also looked into, with X-ray CT scans focusing on the intersection of the tows. The long-term viability of the TWF composite under mechanical and thermal environment is thus verified, and the possibility of the immediate prediction of the final failure under cyclic loading is also discussed.

2 Experimental Procedures

2.1 Materials and Specimens

The close-up of typical TWF composite is shown in Fig. 1. In the present study, two types of TWF composites are prepared and subjected to experiments (Table 1). SK-802 is the combination of T300-1K carbon fiber (Toray Industries Inc.) and 180°C-cure NM35 epoxy resin (Nippon Oil Corp.). SK-803 is the TWF composite combined T-300-2K (Toray Industries Inc.) with the same epoxy resin. The major difference is thus the thickness of the tows which results in the thickness of the composites, with SK-803 approximately twice as thick as SK-802. Fiber volume fractions are also slightly different, 65% and 63% for SK-803 and SK-802, respectively. The manufacturing procedure of both TWF composites is: (1) dry carbon fabric is woven to form a base TWF, (2) resin is impregnated to fabricate a prepreg, (3) single-ply composite plate is cured from this prepreg under autoclave environment. The fabrication and curing procedures are all conducted at Sakase Adtech.

Due to the specific feature of the fabrication process, the manufactured roll of the TWF has one of its tows aligned in the transverse direction of the roll. As a result, the final component formed from the TWF composite usually consists of the tows, one of which is running transverse to its major or the longitudinal direction. The specimens prepared thus have one of the tows aligned in the transverse direction to comply with the ordinary usage of the composite (Fig. 2). Rectangular–shaped 0.5mm thick aluminum tabs are bonded on both ends of the specimens. The gauge length L_G and the width W are 50mm and 25 mm, respectively. Following the usual notation of the fiber angles, the present specimen with one of the tows placed perpendicular to the loading direction is designated as [30/-30/90] specimen, or in an abbreviated form, 90-deg specimen (Fig. 1). The one that has its tow aligned in the loading direction is then designated as [0/60/-60] specimen, which will not be adopted herein.

2.2 Experimental Setups

Static tensile and cyclic tensile tests on TWF composite are performed using a linear motor testing machine (INSTRON ElectroPuls E10000) at room temperature (RT, 23°C). To determine the cyclic tensile load levels, the static tensile fracture strength is first evaluated. The static tests are carried out under displacement control. The cross-head speed is 0.1mm/min. The cyclic tests are then performed under load control. The tensile load ratio R (=minimum tensile load / maximum tensile load) is kept at a constant value of R=0.1. Cyclic loading is applied by a sinusoidal waveform whose frequency is 10Hz.

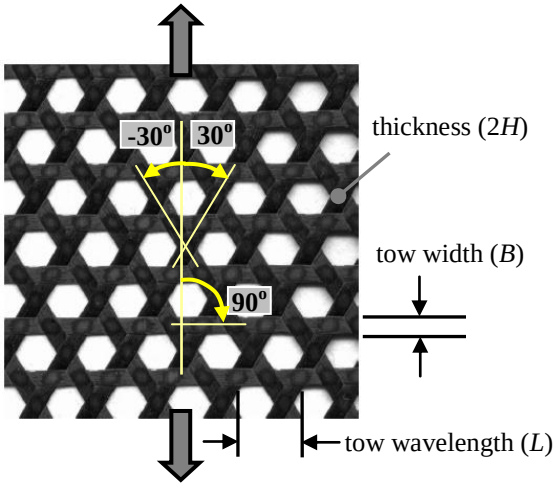

Fig. 1. Close-up view of TWF composite (portion of [30/-30/90] or 90deg specimen)

Table 1 Properties of TWF composite

type specification	SK-802	SK-803
fiber	T300-1K	T300-2K
resin	Epoxy NM35	Epoxy NM35
tow width B (mm)	0.90	0.90
tow wavelength L (mm)	3.12	3.12
thickness $2H$ (mm)	0.14	0.24
fiber vol. fraction V_f(%)	63	65

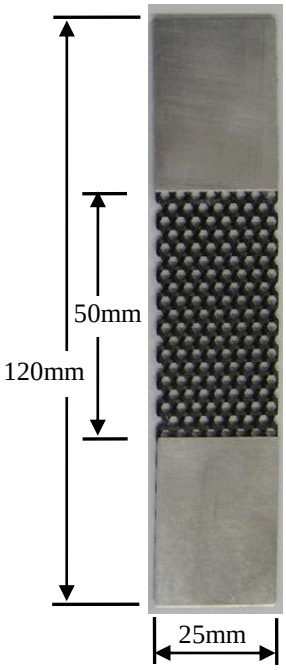

Fig. 2. Specimen configuration

Loaded specimens are subjected to X-ray CT scanning to investigate the damage propagation mechanism of TWF composite after cyclic test at predetermined loading cycles. As the damage propagation in cyclic tests is expected to be quasi-static compared to the rapid damage development in static tests, the damage propagation and accumulation mechanism may possibly be more closely observed. The X-ray CT scanning is performed using TOSHIBA TOSCANER-30000 μ uhd. In this study, ZnI_2 penetrant is applied to emboss the debonded regions.

3 Experimental Results and Discussions

3.1 Static Tensile Fracture Strength and Fracture Characteristics

Three specimens are subjected to the static tensile fracture tests. The results are plotted in terms of equivalent resultant force (N/mm) versus strain in Fig. 3(a), and tangent stiffness (kN/mm) versus strain in Fig. 3(b). The equivalent resultant force is defined as the value of the tensile force divided by the specimen width and the strain as the specimen elongation divided by the specimen gauge length, respectively. The obtained average tensile fracture strengths are 20.0 (N/mm) for SK-802 and 29.2 (N/mm) for SK-803. The corresponding average tensile fracture strains are 1.09 and 1.03 and the initial tangent stiffness are 1.9 and 3.5 (kN/mm). The average tensile fracture strength of SK-803 is about 1.5 times that of SK-802 and the ratio of initial tangent stiffness is about 1.8. Both the tensile fracture strength and tangent stiffness of SK-803 are expected to be approximately twice the values of SK-802, as the fiber density for SK-803 is apparently twice that of SK-802. Thus the inherent static properties of fibers are more efficiently realized with SK-802 than with SK-803.

These experimental results can be explained by the difference in the degree of crimp of the tows. Once the sinusoidal out-of-plane displacement of the tow is assumed, the crimp ratio *CR* of the tow is defined as $CR=H/L$, where H is the local thickness of the single tow and L the wavelength of the waviness. As a result, *CR* represents the measure of the local crimp of the tows. In this case, CR=0.022 and 0.038 for SK-802 and SK-803, respectively. Crimp ratio *CR* corresponds to the amount of tow bending and

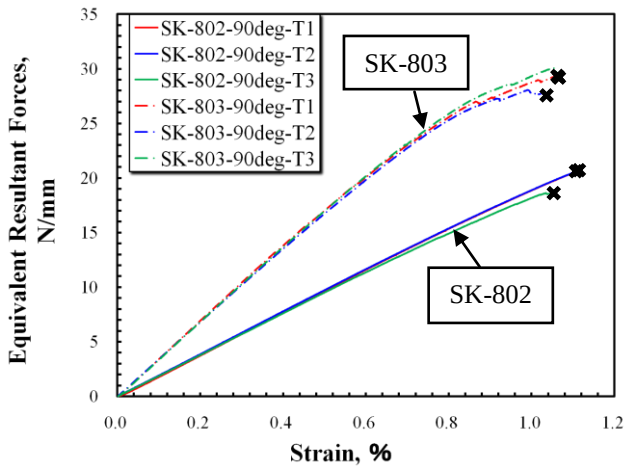

(a) Force vs. strain

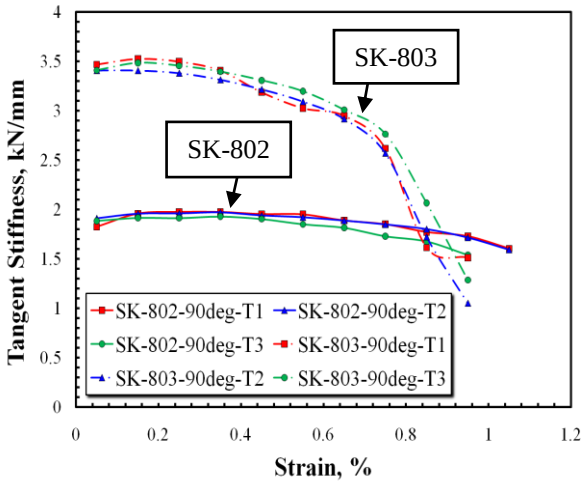

(b) Tangent stiffness vs. strain

Fig. 3. Static tensile test results

twisting at the tow overlaps (Fig. 4) and the intensive stress concentration inevitably takes place at these portions. Thus the tensile strength of SK-803 may not achieve as high as expected based on the results of SK-802. Crimp may also affect the tangent stiffness of the composite as the in-plane effective stiffness of the tows decreases with increasing crimp rate.

Another obvious difference is observed in the force versus strain behavior, which may be suggesting the distinction of damage formation characteristics. From Fig. 3, the first local failure is inferred to have occurred at the strain level of ε=0.8 for SK-803, as the stiffness rapidly decreases above this strain level. On the other hand, there is little reduction in the

stiffness of SK-802 and the final fracture suddenly takes place when strain approaches ε=1.1. These results indicate that the damage accumulates moderately in SK-803, while relatively abrupt damage accumulation takes place in SK-802. It can so far be speculated that the damage susceptibility of TWF composite is strongly affected by the fiber filament number. Increase of fiber filament may be resulting in the higher capability of carrying the diverted stress flow when the local failure occurs. Thus, it is more probable that SK-803 exhibits the apparently 'ductile' type of characteristics compared to the 'brittle' behavior of SK-802.

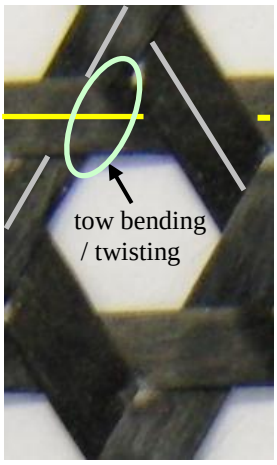

Fig. 4. State of tow bending / twisting at the overlaps

3.2 S-N Diagrams

Figure 5 shows the S-N diagram obtained from the cyclic tests. Number of cycles at failure N_f is plotted against the maximum cyclic tensile load. The static tensile strength obtained above are also plotted on the vertical axis at N_f =1 of the S-N diagram. The endurance limits of both materials are not observed up to 10^6 cycles region. The figure also indicates that the relationships for both SK-802 and SK-803 can be approximated as linear relations at least up to 10^6 cycles loading.

The effect of hygrothermal environment is also considered. In Fig. 6, number of cycles at fracture is plotted for different temperature environment under maximum cyclic stress set constant to 60% of the average static tensile strength (60% UTS). The data set shown in the figure is under 50% relative humidity.

3.3 Trends of Maximum Strain under Cyclic Loading

The trends of the maximum cyclic strain are plotted against the logarithm of the number of cycles in Fig. 7. The figures exhibit that creep or ratchet phenomenon takes place during the cyclic tests of both materials. The time average of the stress is well above zero in the present tensile cyclic tests and thus

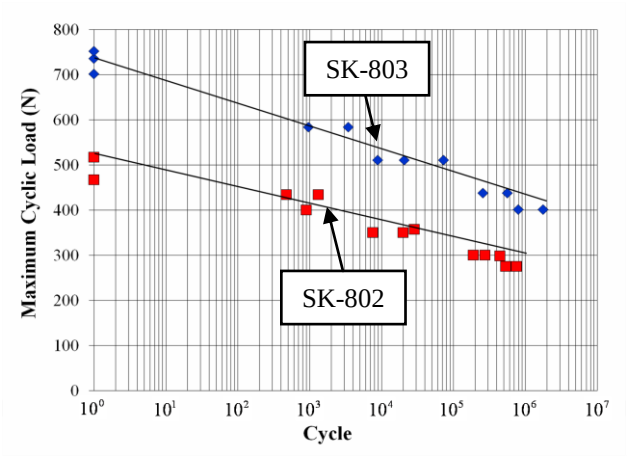

Fig. 5. S-N diagram

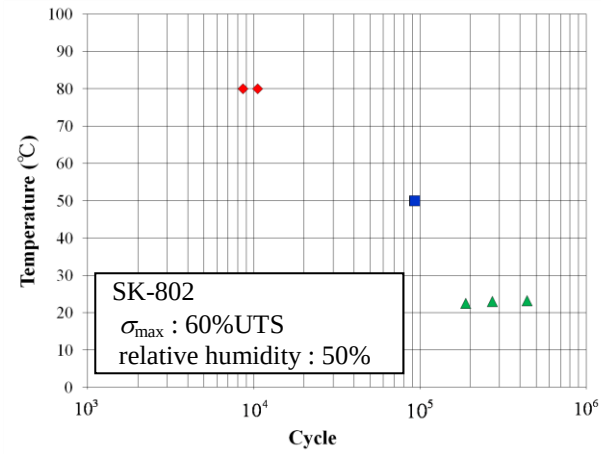

Fig. 6. Thermal effect on the fatigue strength

this behavior may well be expected. Both materials have certain threshold strain values beyond which the rapid strain extension occurs, and these thresholds vary with loading levels. This acceleration behavior of the strain increase is different for SK-802 and SK-803. For SK-803, the cyclic strain growth after the threshold is very large compared to that of SK-802. Therefore, it can be inferred that the fatigue fracture evolution characteristic of SK-803 is more stable than SK-802. This corresponds to the static test results in which SK-803 behaved as relatively 'ductile' material system.

3.4 Damage Observation by X-ray CT Scanning

Fractured specimens after the tests are shown in Fig. 8. Although each specimen has undergone different levels of maximum cyclic load, the fractured patterns of specimens are apparently quite similar.

These appearances are also obtained with the dog bone shaped specimens in reference[5] with different dimensions. Therefore, the failure mode of TWF composite may have unique characteristic regardless of the maximum loading levels or specimen geometries. The weakest failure portion of TWF composite is expected to be the adhesive layers at the intersection or overlap of tows, so the initial debonding failure has likely occurred at one of these intersections. This debonding then propagates diagonally along one of the oblique tows and may induce stress increase at adjacent tows that may result in the final failure.

To verify this presumption, the X-ray CT scanning of SK-803 specimens, which undergone different levels of cyclic loadings, is performed. Figure 9 shows the scanned result of through-thickness cross section of specimen that exhibited the maximum tensile strain of $\varepsilon_F = 0.9$ (slightly before the fracture). The result represents that the debondings occur at the tow intersections indicated with the yellow circles. Furthermore, it is observed that the debonding points lie on the identical diagonal tow line from bottom left to top right and this result corresponds to the failure mode shown in Fig. 8. Thus, the presumption that the debonding at the tow intersection strongly affects the overall fracture is highly probable. However, the initial failure point is not specified so far. The finite element analysis is also conducted which provides indications of portions of extreme stress concentrations, which gives the additional support for the above indicated failure mechanism.

4 Concluding Remarks

Fatigue behavior of TWF composite and its damage propagation and accumulation mechanisms are experimentally investigated. Two types of TWF composites with different filament thickness are employed. S-N curves for these composites are constructed and the strain increment or ratcheting behavior under cyclic loading is investigated. The results reveal that the difference in filament number of fiber tows used affects the damage accumulation rates and the resulting final failures. The one with thicker tows behaves as more 'ductile' material. Tow debonding, which is suspected to be the major initial damage, is also observed using X-ray CT scanning. Both composites exhibit similar fracture

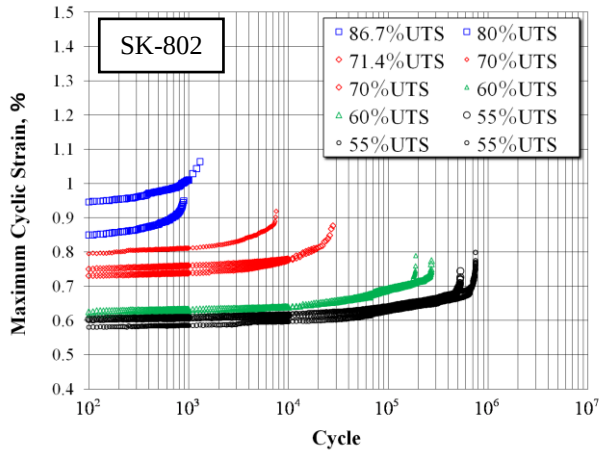

(a) SK-802

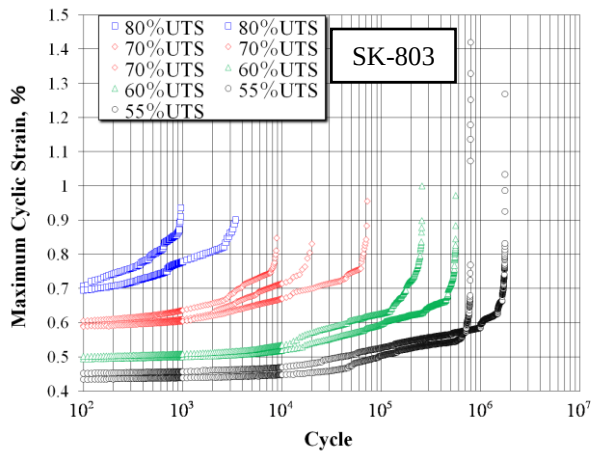

(b) SK-803

Fig. 7. Trends of maximum strains under constant cyclic loading

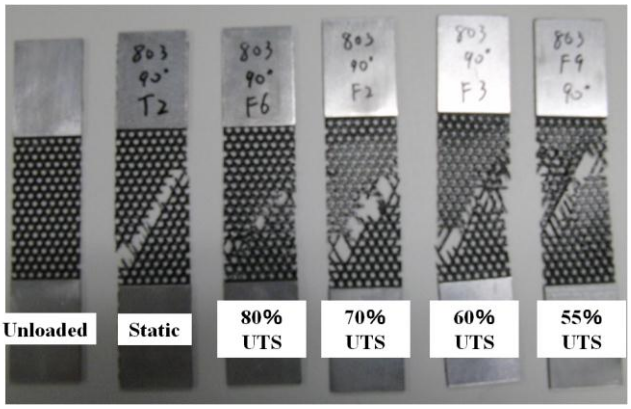

Fig. 8. Fractures specimens under static and cyclic loadings (SK-803)

mode for cyclic as well as static loadings. The precise failure mechanism is still under investigation, and in this context the FE analyses are conducted to identify the portions of stress concentrations where initial failure may likely take place.

References

[1] Yoshida K., Ph.D Thesis, University of Tokyo, 2007, in Japanese.

[2] Aoki, T. and Yoshida, K., "Mechanical and Thermal Behaviors of Triaxially-Woven Carbon/Epoxy Fabric Composites," AIAA-2006-1688, 47th *AIAA/ASME/ ASCE/AHS/ASC Structures, Structural Dynamics, and Materials Conference*, 2006.

[3] Aoki, T. and Yoshida, K., "Feasibility Study of Triaxially-Woven Fabric Composite for Deployable Structures," AIAA-2007-1811, *48th AIAA/ASME/ ASCE/AHS/ASC Structures, Structural Dynamics, and Materials Conference*, 2007.

[4] Fujita, A., Hamada, H., and Maekawa, Z., "Tensile Properties of Carbon Fiber Triaxial Woven Fabric Composites," *Journal of Composite Materials*, vol. 27, pp.1428-1442, 1993.

[5] Dano, M.L., Gendron, G., and Picard, A., "Mechanical Behavior of a Triaxial Woven Fabric Composite," *Mechanics of Composite Materials and Structures*, vol. 7, pp.207-224, 2000.

[6] Zhoa, Q., and Hoa, S.V., "Triaxial Woven Fabric (TWF) Composites with Open Holes (Part I): Finite Element Models for Analysis, " *Journal of Composite Materials*, vol. 37, pp.763-789, 2003.

[7] Nakatani, I., Tsuruda, K., and Yamamoto, T. "PLANE-B: Mars mission with small spacecraft but potentially with large science reward," *Acta Astronautica*, vol. 35, pp.337-344, 1995.

[8] Kawaguchi, J., Fujiwara, A., and Uesugi, T., "Hayabusa - Its technology and science accomplish -ment summary and Hayabusa-2," *Acta Astronautica*, vol. 62, pp.639-647, 2008.

[9] Higuchi, K., Watanabe, K., Watanabe, A., Tsunoda, H., and Yamakawa, H. "Design and Evaluation of an Ultra-Light Extendible Mast as an Inflatable Structure," AIAA-2006-1809, *47th AIAA/ASME/ ASCE/AHS/ASC Structures, Structural Dynamics, and Materials Conference*, 2006.

[10] Obst, A., Palermo, G., Ticci, L., and Santiago Prowald, J., "Modeling of triaxial woven fabrics for antenna reflectors," *Proceedings of the European Conference on Spacecraft Structures, Materials and Mechanical Testing 2005 (ESA SP-581)*, 2005.

[11] Aoki, T. et. al., "On-Orbit Verification of Space Inflatable Structures," *Proceedings of the 26th International Symposium on Space Technology and Science*, Hamamatsu, Shizuoka, Japan, June 2-8, 2008.

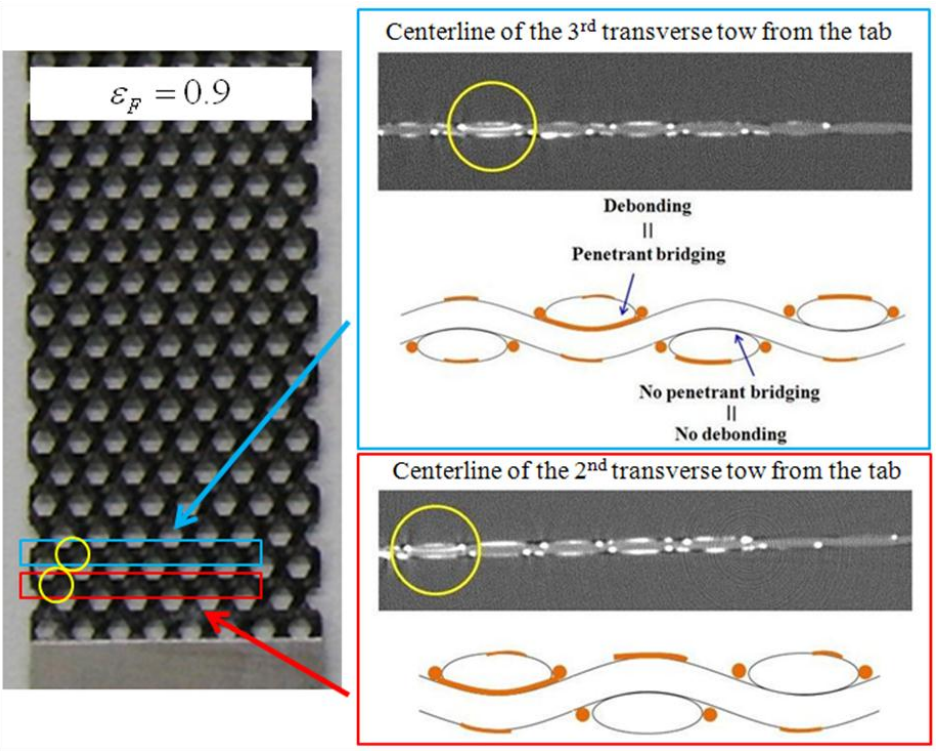

Fig. 9. X-ray scanning results of specimen subjected to high tensile strain (SK-803, through-thickness cross section)